ICIC Express Letters
Volume **10**, Number **7**, July **2016**

 ISSN 1881-803X
pp. **1581–1589**

A CALCULATION METHOD FOR TORQUE OF MAGNETIC COUPLING

Cunhe Li, Guofeng Wang, Yongsheng Zhao and Yunsheng Fan

College of Information Science and Technology
Dalian Maritime University
No. 1, Linghai Road, Dalian 116026, P. R. China
licun.he@163.com

Received December 2015; accepted March 2016

Abstract. *This paper presents an approach for quick calculation of the torque of magnetic coupling. Through analyzing the magnetic field characteristics of magnetic coupling, the equivalent magnetic circuit model is established. Based on equivalent magnetic circuit model, the torque calculation formula for the magnetic coupling is deduced. Finally, the proposed calculation method is validated with 3-D finite element simulation and with experimental results.*
Keywords: Magnetic coupling, Equivalent magnetic circuit, Torque calculation formula, Finite element

1. **Introduction.** With the rapid development of permanent magnetic materials, magnetic couplings have been widely applied in the modern industry. The magnetic couplings are able to finish the transmission of a torque from the prime mover to the load without any mechanical contact. They achieve the good effect by reducing the noise and easing the vibration, and they can avoid the damage caused by the system when the motor shaft and the load shaft cannot accurately align [1,2]. The transmitting torque plays an important role in predicting the performance of magnetic coupling [3]. The mathematical model of transmitting torque can reflect the relationship between the transfer capability and design parameters. Therefore, the research on the mathematical model of transmitting torque has important theoretical and practical significance.

There are many research results for the calculation of torque of magnetic coupling. Formal design optimization of magnetic coupling is represented using a layer model approach [4]. The analysis and design of magnetic coupling using a pure analytical procedure are showed based on variable separation method [5]. The analytical calculations for torque and axial force of magnetic coupling are presented with the equivalent magnetic charge method [6]. The spatial distribution of the air-gap magnetic field in the magnetic coupling is described using the formula of theoretical arithmetic on air-gap magnetic field based on the equivalent surface current model [7]. The magnetic flux density distribution, eddy currents density distribution and the influence of various design parameters for the torque of magnetic coupling are represented using the finite element analysis [8,9].

The objective of this paper is focused primarily on the use of analytical method to calculate the torque of magnetic coupling. Firstly, the equivalent magnetic circuit model has been established according to the magnetic field characteristics of magnetic coupling. Then the torque calculation formula has been derived. Furthermore, the simulation model of magnetic coupling is established and analyzed by the use of the finite element analysis software. Finally, an experimental platform is built and the validity of analytical method is verified through the experimental test.

2. **Mechanical Structure and Operation Principle.** The basic structure of magnetic coupling is shown in Figure 1. The main components of magnetic couplings are a Magnet Rotor that is surrounded by a Conductor Rotor. The Magnet Rotor assembly is made of one magnet disc that contains powerful rare-earth magnets. The Magnet Rotor is usually mounted to the load shaft. The Conductor Rotor assembly is made of a fabricated steel housing with copper conductor rings attached to the inside surface facing the Magnet Rotor. The Conductor Rotor assembly is usually mounted to the motor shaft. The Magnet Rotor and Conductor Rotor are never in contact with each other.

If the Conductor Rotor has a velocity relative to the Magnet Rotor, then the eddy currents will be produced based on the slip on the copper conductor rings. The induced eddy currents within the skin depth of the conductors generate an induced magnetic field. The interaction between induced magnetic field and permanent magnetic field will result in a circumferential resultant force such that the Magnet Rotor will endeavor to catch up with Conductor Rotor. Through this coupling between Conductor Rotor and Magnet Rotor, the energy transfer is achieved.

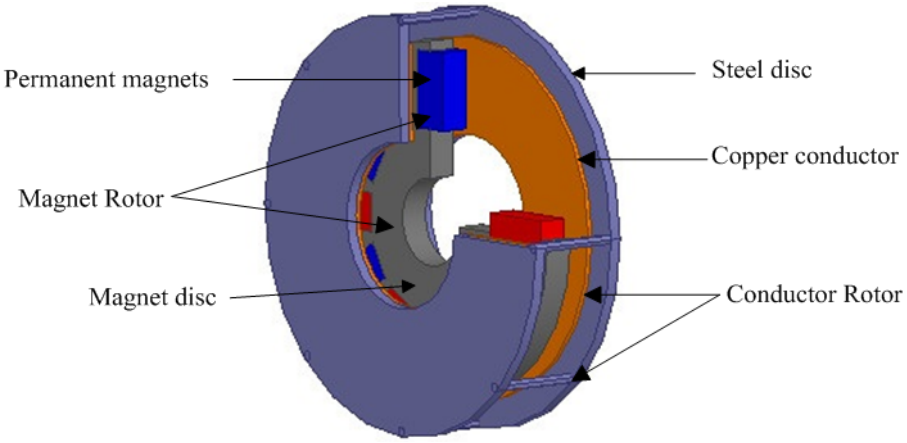

FIGURE 1. The mechanical structure of magnetic coupling

3. Calculation Method.

3.1. **Equivalent magnetic circuit model.** The magnetic flux path of magnetic coupling is shown in Figure 2(a). Because the coupling process of magnetic coupling running is complex, we make following assumptions: (1) ignore the effect of temperature on the conductivity and permeability; (2) material is isotropic; (3) ignore hysteresis effect.

Based on the above assumptions, the equivalent magnetic circuit model for magnetic coupling can be established which is shown in Figure 2(b). The effective magnetic circuit is an air reluctance, copper conductor rings reluctance and steel disc reluctance in series. Considering the influence of leakage flux, the leakage reluctance and reluctance of effective magnetic circuit are parallel. The pair of magnetic poles of the magnetic circuit can be further simplified as a magnetic pole of the magnetic circuit, where the simplified magnetic circuit is shown in Figure 2(c).

The steel disc is made of high permeability materials. Its reluctance is far less than other and can be ignored. So the total reluctance of a magnetic pole could be expressed in the following:

$$R_t = \frac{2R_l(R_a + R_c)}{R_a + R_c + R_l} + R_m \tag{1}$$

where R_a is the air-gap reluctance, R_c is the copper conductor reluctance, R_l is the leakage reluctance, and R_m is the permanent magnet reluctance.

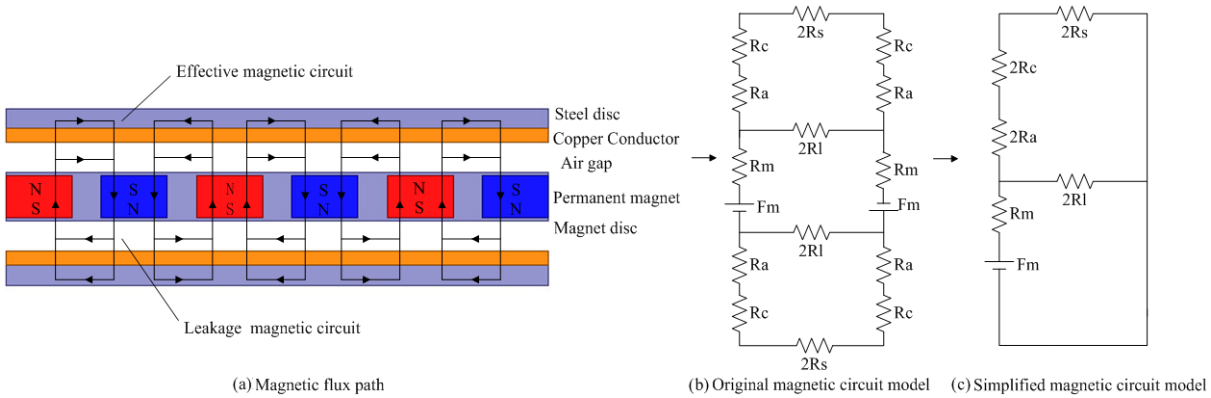

FIGURE 2. The equivalent magnetic circuit model of magnetic coupling

Furthermore, the magnetic permeability of air gap, copper conductor and permanent magnet is approximately 1. According to the formula of the reluctance $R = l/(\mu S)$, the reluctance can be separately calculated as follows:

$$R_a = l_a/(\mu_0 S_m), \quad R_c = l_c/(\mu_0 S_m), \quad R_l = l_b/\left(2\mu_0 l_a\sqrt{S_m/\pi}\right), \quad R_m = l_m/(\mu_0 S_m) \tag{2}$$

where l_a is the length of air gap, l_c is the thickness of copper conductor, l_b is the average length of adjacent magnetic circuits, l_m is the thickness of permanent magnet, μ_0 is the magnetic permeability of vacuum, and S_m is the cross-sectional area of permanent magnet.

3.2. **Torque calculation.** In the calculation of the torque, it is assumed that the shape of the eddy current region is approximately circular and equals $1.0 \sim 2.0$ times of the cross-sectional area of the permanent magnet. The ratio of eddy current area to cross-sectional area of magnet is defined as

$$k_c = S_e/S_m \tag{3}$$

where S_e is the area of eddy current region, $S_e = \pi(d/2)^2$, and d is the diameter of the circular area.

A permanent magnet is taken as an example. The corresponding eddy current region in the copper conductor is circular. With the rotation of the drive rotor, changing rule of magnetic flux of the circular area can be considered to be sine regularity [10] as

$$\Phi = BS_e \sin w_p t \tag{4}$$

where w_p is the angular velocity, $w_p = 2\pi pn/60$, p is the pairs of magnetic pole, n is the slip, t is the run time, and B is the air-gap magnetic flux density.

According to the law of electromagnetic induction, the alternating magnetic field will generate the induced electromotive force, which can be calculated by

$$\varepsilon = d\Phi/dt = BS_e w_p \cos w_p t \tag{5}$$

Due to the skin effect of eddy currents, many eddy currents rings with radius being r, width dr and skin depth Δ_h (when the skin depth is greater than the thickness of copper conductor, Δ_h represents the thickness of copper conductor) are formed on the copper conductor on one near side of the permanent magnet as shown in Figure 3.

The resistance of eddy current ring is

$$dR = 2\pi r\rho/(\Delta_h dr) \tag{6}$$

where ρ is the resistivity of Cu, r is the radius of eddy current rings and Δ_h is the skin depth, $\Delta_h = \sqrt{2\rho/(w_p\mu_0)}$.

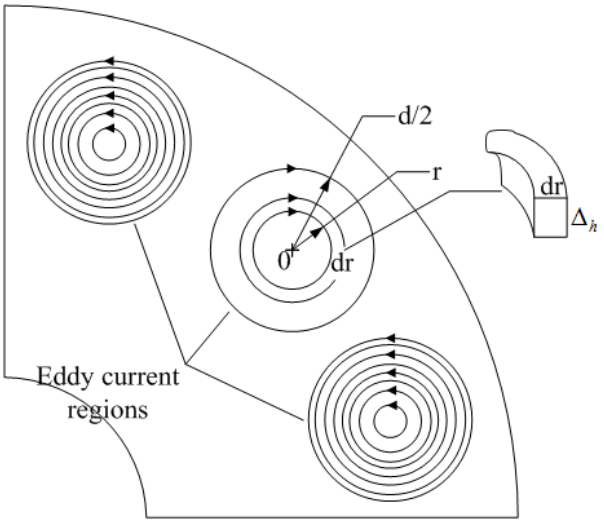

FIGURE 3. The diagram of eddy current region

The transient eddy current value with a single permanent magnet is derived as

$$i = \int_0^{\frac{d}{2}} di = \int_0^{\frac{d}{2}} \frac{\varepsilon}{dR} = \frac{\Delta_h B w_p S_e \cos w_p t}{4\pi\rho} \tag{7}$$

So the effective value of eddy current could be expressed in the following:

$$i_e = \frac{i_{\max}}{\sqrt{2}} = \frac{\sqrt{2}\Delta_h B w_p S_e}{8\pi\rho} \tag{8}$$

Furthermore, the eddy current losses of all permanent magnets in a cycle are calculated by

$$P = k\frac{1}{T_c}\int_0^{T_c}\int_0^{\frac{d}{2}} dPdt = k\frac{1}{T_c}\int_0^{T_c}\int_0^{\frac{d}{2}} \frac{\varepsilon^2}{dR}dt = \frac{k\Delta_h B^2 w_p^2 S_e^2}{16\pi\rho} \tag{9}$$

where k is the number of permanent magnet poles, and T_c is the cycle.

The eddy current of copper conductor rings generates a strong induced magnetic field during its runtime. It will produce a strong demagnetizing effect. The total magnetomotive force can be expressed as

$$F = F_m - F_e, \quad F_m = H_m l_m, \quad F_e = k_e i_e \tag{10}$$

where F_m is the magnetomotive force of a magnet pole, H_m is the coercivity of permanent magnet, F_e is the induced magnetomotive force of eddy currents, k_e is the convert coefficient of eddy currents and usually taken 1.5 and i_e is the effective value of eddy currents.

According to the magnetic Ohm's law, the magnetic flux of magnetic circuit can be determined as

$$\Phi = BS_m = \frac{FR_l}{R_t(R_a + R_c + R_l)} \tag{11}$$

Thus, the air-gap flux density can be obtained as follows:

$$B = \frac{\Phi}{S_m} = \frac{8\pi\rho H_m l_m R_l}{8\pi\rho S_m R_t\left(R_a + R_c + R_l\right) + \sqrt{2}k_e\Delta_h w_p S_e R_l} \tag{12}$$

Substituting Equation (12) into Equation (9), the power can be rewritten as follows:

$$P = \frac{4\pi\rho k\Delta_h w_p^2 k_c^2 H_m^2 l_m^2}{\left[8\pi\rho\frac{R_t}{R_l}\left(R_a + R_c + R_l\right) + \sqrt{2}k_e\Delta_h w_p k_c\right]^2} \tag{13}$$

Finally, the torque of magnetic coupling can be calculated as follows:

$$T = \frac{P}{w_n} = \frac{4\pi\rho k \Delta_h w_p^2 k_c^2 H_m^2 l_m^2}{w_n \left[8\pi\rho \frac{l_b S_m (2l_a + 2l_c + l_m) + 2l_m l_a \sqrt{S_m/\pi}(l_a + l_c)}{\mu_0 l_b S_m^2} + \sqrt{2} k_e \Delta_h w_p k_c \right]^2} \tag{14}$$

where w_n is angular velocity of rotating machinery, $w_n = 2\pi n/60$.

4. The Simulation Analysis and Experiments.

4.1. **Simulation analysis.** A magnetic coupling prototype whose rated output power is 45 KW and rated output speed is 1475 rpm, as shown in Figure 4(a), was built where the rectangle-shaped NdFeB magnets were mounted in middle magnet disc. Based on the above analysis, build the prototype's 3-D finite element (FE) model as shown in Figure 4(b). The design and material parameters are given in Table 1. Let the air gap have a 3mm length, the performance of magnetic coupling can be simulated through finite element analysis (FEA).

Through simulation, magnetic flux density map of the copper conductor could be obtained. Figure 5 shows magnetic flux density distribution of static. It could be seen the number of magnet poles induced in the copper conductor is 10, equal to the number of magnet poles. Magnetic flux density decreases from the pole's middle to outer area.

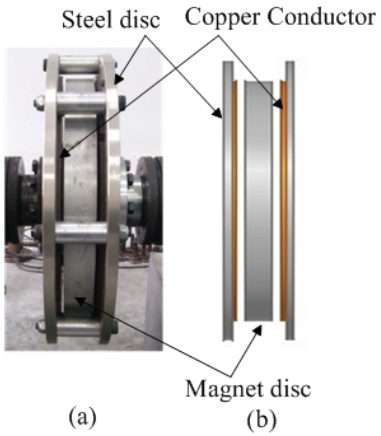

FIGURE 4. Prototype and FE model

TABLE 1. Design and material parameters of FE model

Parameters	Symbol	Value	Unit
Number of pole pairs	p	5	–
Relative permeability of magnet	μ_r	1.099	–
Magnetic permeability of vacuum	μ_0	$4\pi \times 10^{-7}$	H/m
Magnet coercivity	H_m	8.9×10^5	A/m
Magnet thickness	l_m	0.032	m
Magnet area	S_m	0.0029	m^2
Area ratio	k_c	1.4	–
Copper conductor thickness	l_c	0.005	m
Copper conductivity (20°C)	ρ	1.75×10^{-8}	$\Omega \cdot m^2/m$
Steel disc thickness	–	0.01	m
Steel conductivity (20°C)	–	1.75×10^{-8}	$\Omega \cdot m^2/m$

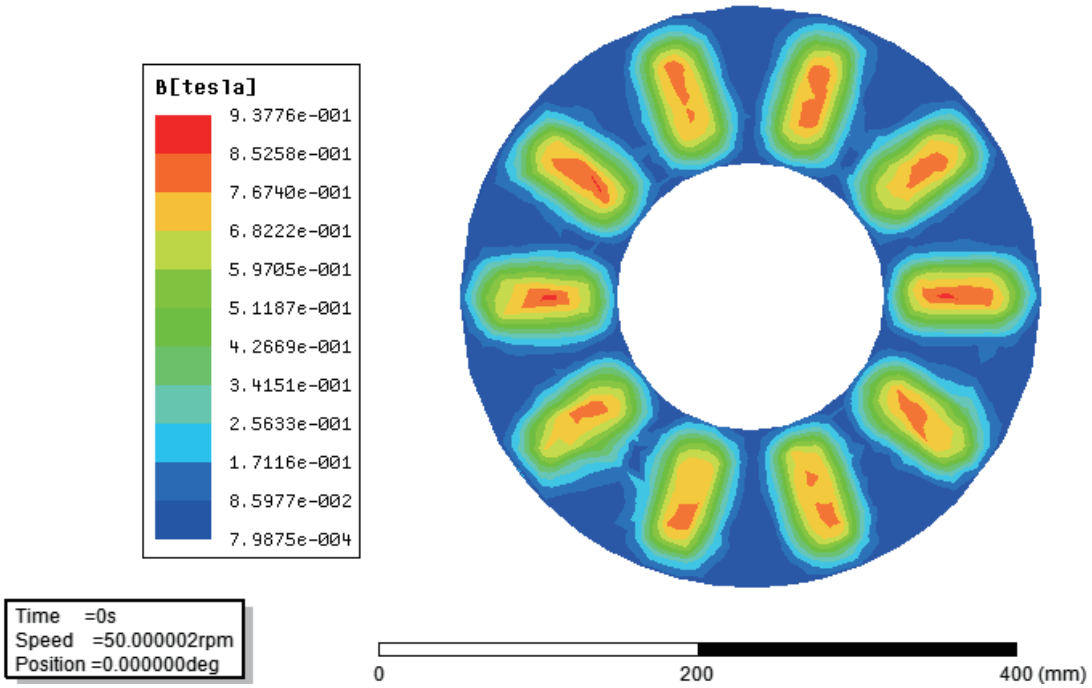

FIGURE 5. Magnetic flux-density map at 0 rpm

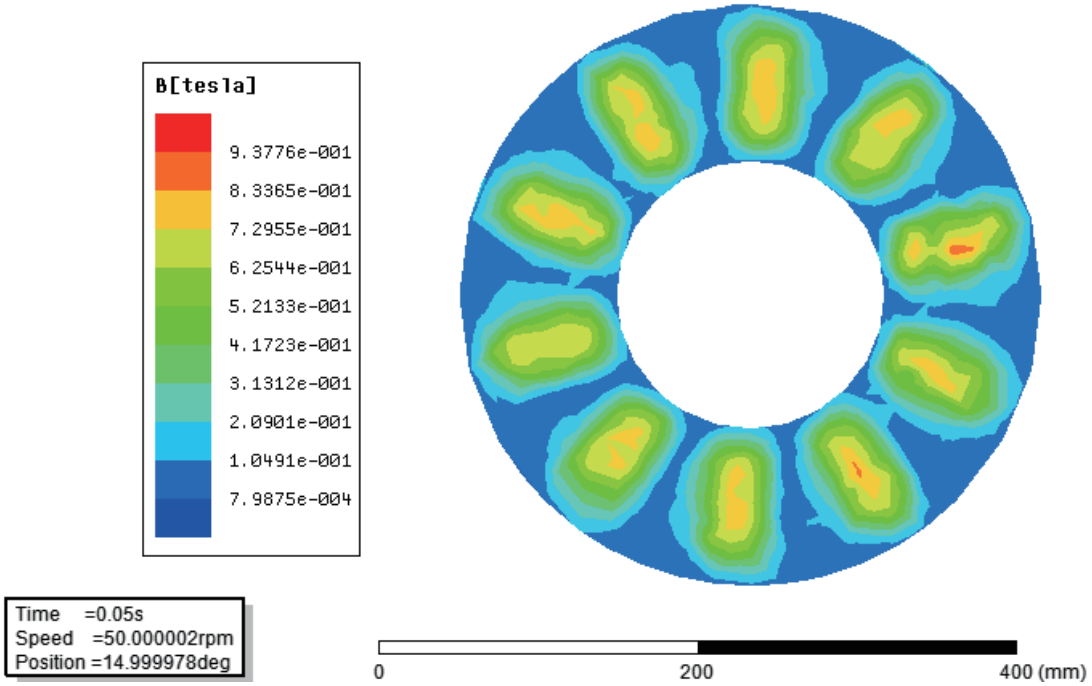

FIGURE 6. Magnetic flux-density map at 50 rpm

Figure 6 shows that the magnetic flux flow in simulated is lower than static because the magnetic field of eddy current produced demagnetization effect.

From Figure 7, it could be seen that the distribution of eddy current is not uniform in the whole copper conductor and the number of maximums is equal to the number of permanent magnets. Every area of eddy current region is approximately equal to $1.0 \sim 2.0$ times of the cross-sectional area of the permanent magnet. This is consistent with the previous assumption in Section 3.2.

The distribution of eddy current density vector on the copper conductor is presented in Figure 8. Eddy current behaves as annular distribution, and there are 10 eddy current

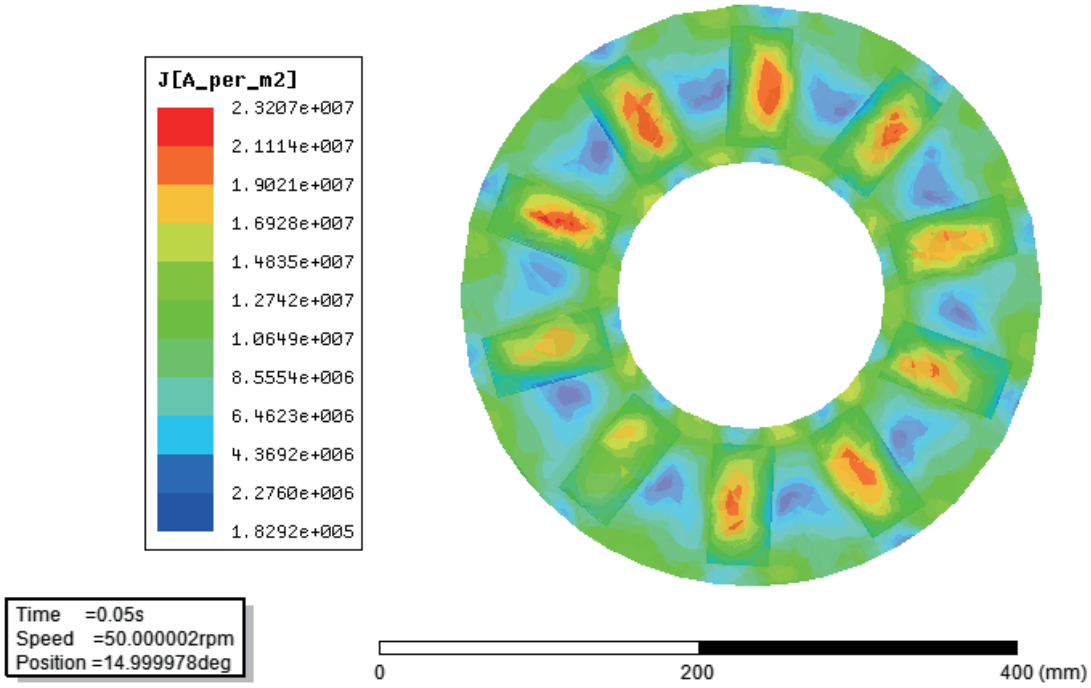

FIGURE 7. Distribution of eddy current density

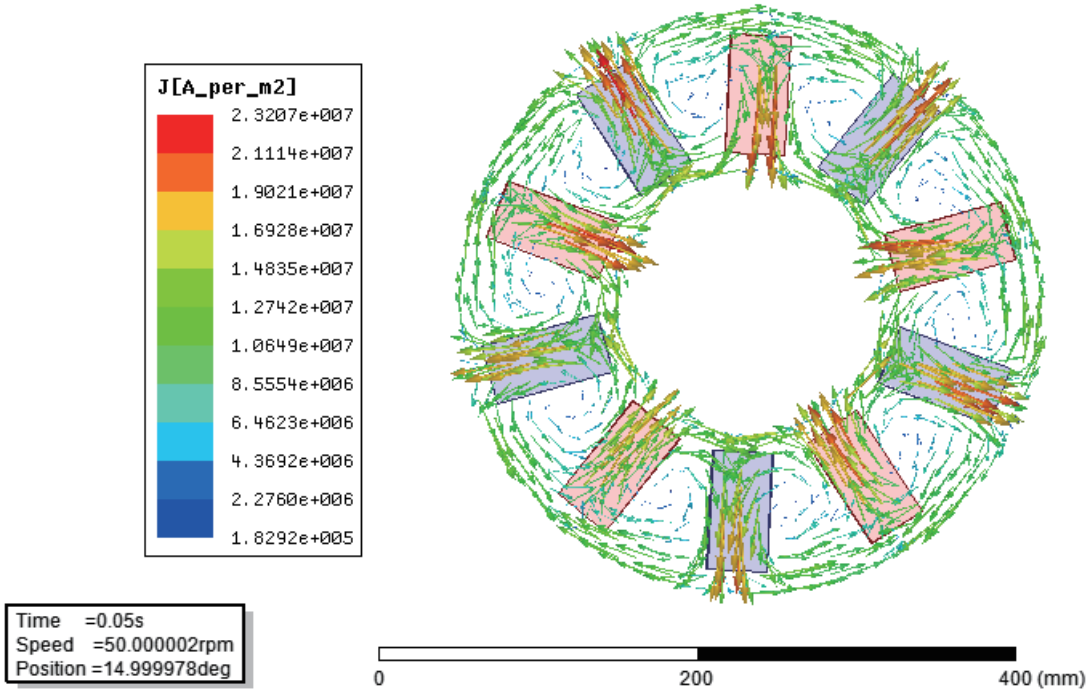

FIGURE 8. Distribution of eddy current density vector

rings in the copper conductor. The current density in the middle of ring is small and the outer part is big.

4.2. **Experiments.** To verify the performance of magnetic coupling prototype, an experimental platform is developed. The main hardware structure of test platform is shown in Figure 9. The motor can be controlled by variable-frequency driver and its speed and output torque can be changed.

Based on the experimental platform, test the prototype's torque transmission capability over the full range of slip speed, 0 to 50, for 5 different air gap settings: 3mm, 5mm,

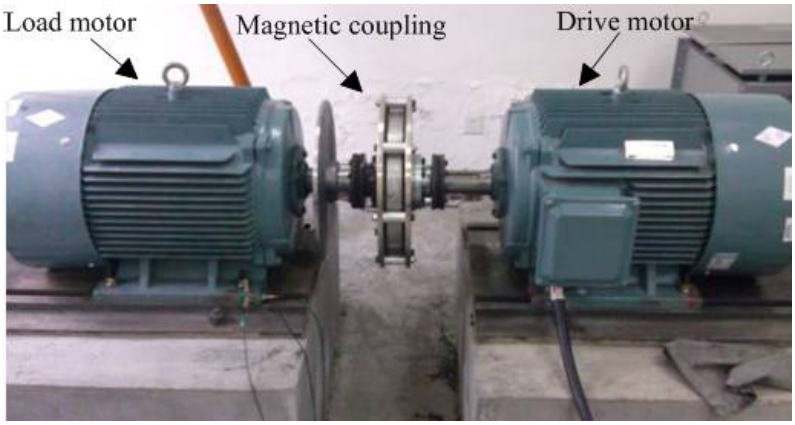

FIGURE 9. Test platform

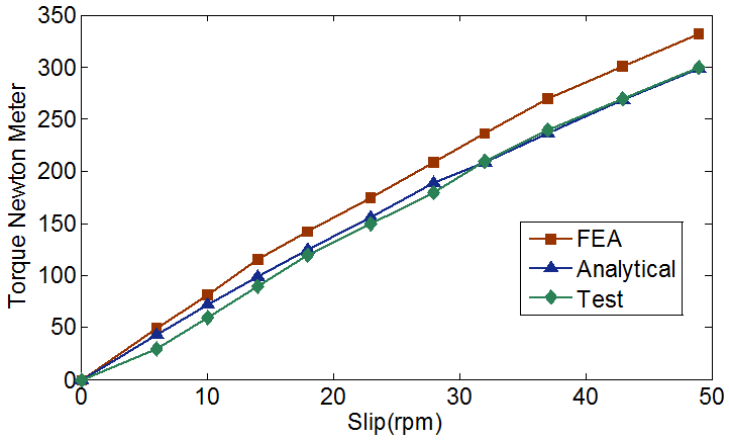

FIGURE 10. Curves of torque with different slip speeds

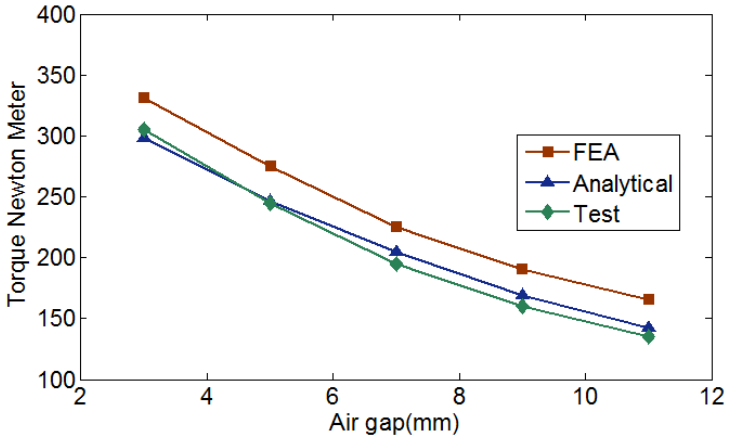

FIGURE 11. Curves of torque with different air gap

7mm, 9mm, 11mm. The results are summarized in Figure 10 and Figure 11. Test the load capacity at different output speeds when air gap is 3mm. Curves of output torque and slip speed were obtained in Figure 10. It could be seen the test results are basically the same with the analytical and simulation results. Keeping the slip speed 50rpm, the curves in Figure 11 demonstrate the inverse air gap relationship for torque.

Compared with finite element analysis value, in summary, the analytical value is closer to the test value in lower slip speed rate. Therefore, the proposed analytical method is proved to be accurate and effective. In addition, finite element analysis needs to establish

the simulation model, whose process is very complex and requires a lot of time. The proposed analytical method can realize the fast calculation of torque for magnetic coupling. The formula can provide a reference for the design and analysis of magnetic coupling.

5. **Conclusions.** A general and practical analytical method has been developed to predict the toque transmission characteristics for magnetic coupling. Comparative studies are carried out between the proposed analytical method, the finite element simulation and test, and the results show that the proposed method is accurate and effective. Because the design parameters are explicit, the proposed analytical method represents a fast analysis tool, and has certain practical significance for design and analysis of magnetic coupling.

Acknowledgment. This work is supported by National High Technology Research and Development Program of China under Grant 2012AA112702, and Fundamental Research Funds for the Central Universities under Grant 3132015039. The authors also gratefully acknowledge the helpful comments and suggestions of the reviewers, which have improved the presentation.

REFERENCES

[1] A. Wallace, C. Wohlgemuth and K. Lamb, A high efficiency alignment and vibration tolerant, coupler using high energy-product permanent magnets, *IEEE Electric Machines and Drives Conference*, vol.73, no.2, pp.232-236, 1995.

[2] J. H. J. Potgieter and M. J. Kamper, Optimum design and comparison of slip permanent-magnet couplings with wind energy as case study application, *IEEE Trans. Industry Application*, vol.50, no.5, pp.3223-3234, 2014.

[3] T. Lubin and A. Rezzoug, Steady-state and transient performance of axial-field eddy-current coupling, *IEEE Trans. Industrial Electronics*, vol.62, no.4, pp.2287-2296, 2015.

[4] A. C. Smith and A. Wallace, Formal design optimization of PM drive couplings, *IEEE the 7th Electric Motors and Drives Conference*, 2002.

[5] A. Canova and B. Vusini, Design of axial eddy-current couplers, *IEEE Trans. Industry Applications*, vol.39, no.3, pp.725-733, 2003.

[6] Z. Wang, Z. Deng and Y. Wang, Numerical calculation for the transmission torque of radical magnetic coupling, *J. Magn. Mater. Devices*, vol.38, no.2, pp.40-43, 2007.

[7] C. Yang, C. Guan, Y. Xu and Y. Hu, Theoretical arithmetic and experimental study on 3D air gap magnetic field for axial asynchronous permanent magnet couplings, *Electric Machines and Control*, vol.17, no.1, pp.51-57, 2013.

[8] K. Yamazaki, Loss analysis of interior permanent magnet motors considering carrier harmonics and magnet eddy currents using 3D FEM, *IEEE Trans. Magnetic*, vol.2, pp.904-909, 2007.

[9] H. K. Razavi and M. U. Lamperth, Eddy current coupling with slotted conductor disk, *IEEE Trans. Magnetics*, vol.42, no.3, pp.405-410, 2006.

[10] X. Long, B. Zhang and L. She, Eddy brake of Maglev train, *Automatic Measurement and Control*, vol.26, no.9, pp.58-59, 2007.